Combining technologies to create bioactive hybrid scaffolds for bone tissue engineering

Anandkumar Nandakumar, Ana Barradas, Jan de Boer, Lorenzo Moroni, Clemens van Blitterswijk and Pamela Habibovic*

Department of Tissue Regeneration; MIRA Institute for Biomedical Technology and Technical Medicine; University of Twente; Enschede, The Netherlands

Combining technologies to engineer scaffolds that can offer physical and chemical cues to cells is an attractive approach in tissue engineering and regenerative medicine. In this study, we have fabricated polymer-ceramic hybrid scaffolds for bone regeneration by combining rapid prototyping (RP), electrospinning (ESP) and a biomimetic coating method in order to provide mechanical support and a physico-chemical environment mimicking both the organic and inorganic phases of bone extracellular matrix (ECM). Poly(ethylene oxide terephthalate)-poly(buthylene terephthalate) (PEOT/PBT) block copolymer was used to produce three dimensional scaffolds by combining 3D fiber (3DF) deposition, and ESP, and these constructs were then coated with a Ca-P layer in a simulated physiological solution. Scaffold morphology and composition were studied using scanning electron microscopy (SEM) coupled to energy dispersive X-ray analyzer (EDX) and Fourier Tranform Infrared Spectroscopy (FTIR). Bone marrow derived human mesenchymal stromal cells (hMSCs) were cultured on coated and uncoated 3DF and 3DF + ESP scaffolds for up to 21 d in basic and mineralization medium and cell attachment, proliferation, and expression of genes related to osteogenesis were assessed. Cells attached, proliferated and secreted ECM on all the scaffolds. There were no significant differences in metabolic activity among the different groups on days 7 and 21. Coated 3DF scaffolds showed a significantly higher DNA amount in basic medium at 21 d compared with the coated 3DF + ESP scaffolds, whereas in mineralization medium, the presence of coating in 3DF+ESP scaffolds led to a significant decrease in the amount of DNA. An effect of combining different scaffolding technologies and material types on expression of a number of osteogenic markers (cbfa1, BMP-2, OP, OC and ON) was observed, suggesting the potential use of this approach in bone tissue engineering.

Introduction

RP technologies are gaining importance as fabrication techniques for preparation of 3D scaffolds used in various tissue engineering applications. The possibility to design and customise scaffold architecture and hence properties with a high degree of reproducibility has made RP a promising alternative to classical scaffolding technologies. Different RP techniques like fused deposition modeling,[1] selective laser sintering[2] and stereolithography[3] have successfully been used for the fabrication of scaffolds for bone tissue engineering. RP scaffolds can be prepared from different materials like polymers, metals and composites.[1,4,5] Using Computer Aided Design/Computer Aided Manufacturing (CAD/CAM) softwares, the mechanical properties[6] and pore sizes[7] can be controlled. It is also possible to fabricate anatomical shapes[8] by combining and integrating RP techniques with imaging techniques like CT scans, thus offering patient specific solutions.

While RP techniques can be used to create 3D scaffolds with sufficient mechanical strength by controlling overall geometrical design and porosity, they do not yet possess the resolution to fabricate nano- and sub-micrometer structures that can mimic the ECM of a cell. In this regard, ESP is gaining widespread attention. The possibility of creating an ECM-like milieu for cells to attach, grow and proliferate has been the main advantage of this method. High voltage is applied to a polymer solution or a melt to produce non-woven fiber meshes in the nanometres to micrometres range that have been used as scaffolds and delivery vehicles.[9-14] The diameter and morphology of the mesh is influenced by the polymer-solvent system, concentration, flow, collector distance, voltage and ambient conditions like temperature and humidity.[15-18]

In few studies, structurally hierarchical scaffolds (macro to nano level) for bone[19] and cartilage[20] tissue engineering applications have been fabricated. Such an approach ensures that a stable support structure is available through the RP compartment of the construct while the ECM-like mesh produced by ESP provides physical cues for the cells. The electrospun layer can also act as a sieve and entrap cells inside the scaffold thereby increasing seeding efficiency. On the other hand, presence of such a mesh should not compromise supply of nutrients into the scaffold and ingrowth of blood vessels.

Scaffolds for load-bearing applications in bone regeneration should be mechanically stable to provide mechanical support, as
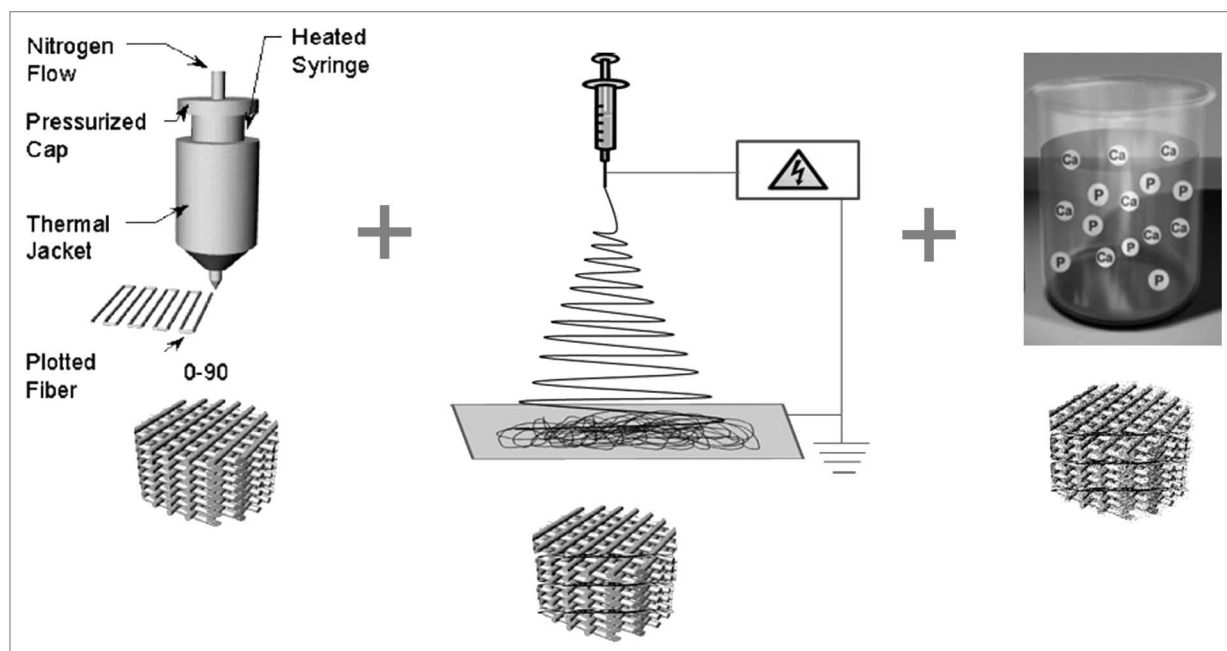
Figure 1. A schematic illustration of the different technologies involved in fabricating the hybrid scaffolds used in this study. (**A**) 3-D fiber deposition (3DF) enables a controlled layer by layer deposition of extruded polymer, (**B**) Electrospinning to produce extra-cellular matrix like fibers and (**C**) Biomimetic calcium phosphate coating to enhance osteoconductivity of the scaffolds.

well as bioactive, facilitating or initiating proliferation and osteogenic differentiation of cells, ECM production and eventually bone deposition. As the inorganic component of bone is primarily composed of calcium-phosphate (Ca-P) in the form of biological apatite, incorporation of Ca-P is another key aspect of scaffold fabrication for bone tissue engineering applications. Ca-P can be added to the bulk material to prepare composite scaffolds or it can be applied as a surface coating. Plasma spraying is the traditional coating method for coating hip implants with hydroxyapatite.[21] Although excellent clinical results were obtained,[22] the process has limitations. The extremely high temperature makes it impossible to coat thermally unstable substrates like polymers or to incorporate biologically active molecules.[23] Plasma spraying only allows for the coating of thermodynamically stable phases and biologically relevant phases like octacalcium phosphate (OCP)[24] and carbonated apatite (CA)[25] cannot be coated by this method. This line-of-sight technique also poses limitations while coating implants or substrates with complex geometrical shapes.[26] Research has led to the development of several other Ca-P coating processes to overcome the limitations of plasma spraying. Among them, biomimetic coating methods involving the immersion of the substrate into solutions simulating physiological fluids are very attractive as the process takes place at near-physiological pH and temperatures, allowing coating of complex and thermally unstable substrates and the incorporation of proteins and growth factors.[27,28] Kokubo et al.[29] developed simulated body fluid (SBF), a solution resembling human blood plasma, in order to study the ability of biomaterials to mineralise in vitro. Based on this, Barrere et al.[30] developed a two-step procedure using a supersaturated solution of SBF (SBF × 5) to coat biomaterial surfaces with a Ca-P layer. Recently, Oliviera and coworkers[31]

used sodium silicate as a nucleating agent and deposited a biomimetic apatite coating on starch-polycaprolactone (PCL) based 3D scaffolds using static and dynamic conditions. Arafat et al.[32] deposited a CA coating in combination with gelatin on PCL/tricalcium phosphate (TCP) 3D scaffolds prepared by a screw extrusion system.

In order to create scaffolds that encompass the required physical and chemical cues for bone tissue engineering applications, in the present study, we combined different technologies, each of which should add a new dimension to the resulting scaffolds. To this end, we used 3DF to create a mechanically stable structure, ESP to provide a random mesh mimicking the ECM and a Ca-P coating to increase bioactivity of polymer used to build the scaffolds. We used a PEOT/PBT block copolymer, commercially sold under the name Polyactive™ (PA), with tunable properties that has been used for various bone,[33] cartilage[34] and osteo-chondral[35] tissue engineering applications before. The biological performance of the hybrid scaffolds developed here was evaluated in vitro by culturing hMSCs and analyzing attachment, metabolic activity and gene expression levels for osteogenic markers.

Results

Fabrication and characterization of scaffolds. A schematic of the fabrication methodology used to produce coated and uncoated 3DF and 3DF + ESP scaffolds is shown in **Figure 1**. Fiber diameter of the scaffolds was 249 ± 21 μm. Fiber spacing and layer thickness were 830 ± 40 μm and 246 ± 22 μm, respectively and these values are in close agreement with the input settings during fabrication. Electrospun meshes consisted
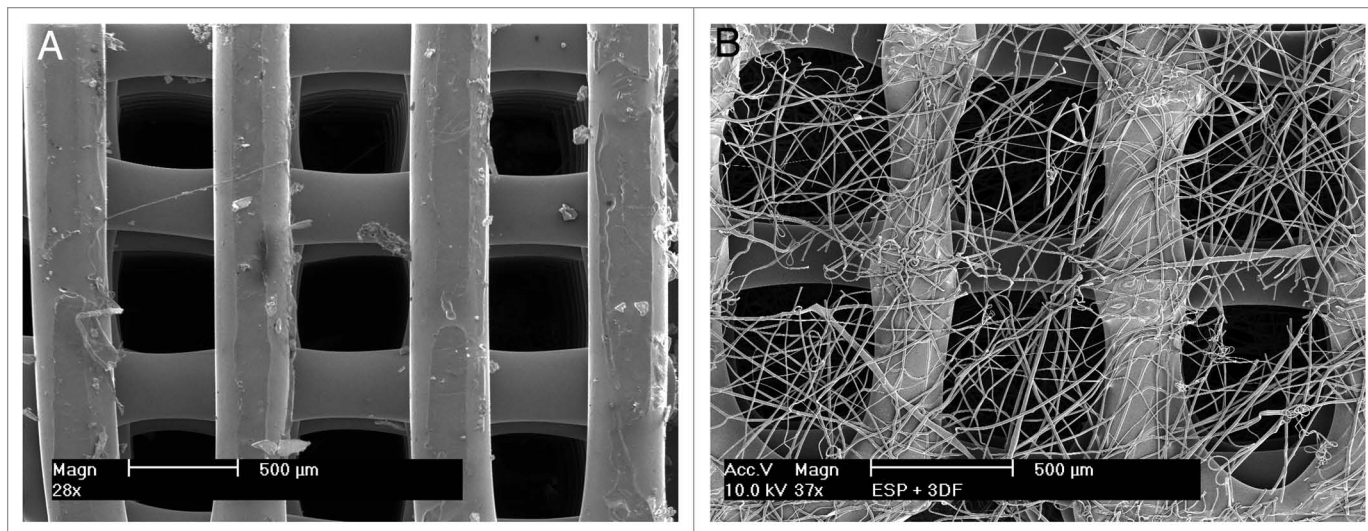
Figure 2. Scaffold morphology using SEM (**A**) 3DF scaffold prepared by rapid prototyping. (**B**) 3DF + ESP scaffold prepared by combining rapid prototyping and electrospinning. The scaffold has been "opened" to enable visualization of the electrospun fiber meshes. Scale bar = 500 μm.

of fibers with a diameter of 5.1 ± 0.94 μm. **Figure 2A** shows a 3DF scaffold while 2B shows an "open" 3DF + ESP scaffold to visualize the concept of combining the two technologies. 3DF and 3DF + ESP scaffolds were coated with Ca-P under near-physiological conditions. The SEM images showing the morphology of the coating, EDX spectrum and mapping for calcium and phosphorus and the FTIR spectrum are presented in **Figure 3**. The SEM images along with the EDX mapping show that the coating homogenously covered the surface of the 3DF scaffolds (**Fig. 3A–D**). **Figure 3E** shows a homogenous distribution of the Ca-P coating on electrospun fibers of the scaffold. The coating consisted of plate-like crystals, with a size of 1–2 μm, orientation of which was perpendicular to the surface of the fibers (**Fig. 3F**). FTIR spectrum of the Ca-P coating indicated mainly the OCP phase. In addition, the spectrum showed incorporation of carbonate into the coating. Typical P-O bands were observed at 562.5 and 602 cm^{-1}. In an earlier study by Du et al.[36] on similar calcium phosphate coatings deposited on PA the bands at 1,104, 1,041 and 960 cm^{-1} were assigned to P-O stretching in PO_4 and HPO_4 group. In the current spectrum, the 1,104 and 1,041 appear to have shifted to 1,114 and 1,040 cm^{-1} while the 960 cm^{-1} band was consistent. Du. et al. also identified carbonate incorporation by bands at 1,467, 1,454, 1,413 and 873 cm^{-1} whereas in the current study, carbonate bands were observed at 1,420, 1,468 and 870 cm^{-1}.

Metabolism and cell numbers. Alamar Blue assay was used to determine the metabolic activity of cells seeded on the different scaffolds. As seen in **Figure 4**, no significant differences were observed between cells seeded on different scaffolds and in different media over time.

On day 21, the amount of DNA present in the scaffolds was analyzed (**Fig. 5**). No significant differences due to the culture media were observed. However the presence of electrospun fibers and coatings had a significant effect on the amount of DNA. In both media, 3DF + ESP + coating showed the lowest DNA

amounts among different scaffold types. When coated scaffolds were compared in basic medium, the presence of electrospun fibers reduced the amount of DNA significantly (3DF + ESP + coating < 3DF + coating). In mineralization medium, 3DF + ESP scaffolds had significantly higher DNA amounts compared with coated scaffolds of the same type.

Cell morphology using SEM. Figure 6 shows SEM images of cell-scaffold constructs cultured in basic medium at 21 d. From the images, it can be observed that cells penetrated into the scaffolds. The retention of cells by the electrospun mesh and the preferential attachment of cells to the fibers compared with the struts of the 3D scaffold can be seen in **Figure 6C**. An open ESP + 3DF scaffold is shown in the inset in C and a cell layer covering the electrospun mesh can be observed. The white arrow points to electrospun fibers. **Figures 6A and F** show the attachment of hMSCs on Ca-P coatings and on electrospun fibers respectively with arrows pointing to calcium phosphate particles and electrospun fibers.

Gene expression analysis using quantitative PCR. The expression of Osteocalcin (OC), Bone Sialoprotein (BSP), Runt-related Transcription Factor-2 (RUNX2/cbfa-1), Collagen type 1 (Col-I), Osteopontin (OP), Osteonectin (ON), and Alkaline Phosphatase (ALP) as markers of osteogenic differentiation was analyzed on days 7 (**Fig. 7**) and 21 (**Fig. 8**) to evaluate the osteogenic potential of the different scaffolds. The fold induction was calculated relative to the expression of the genes on the 3DF scaffold in basic medium. The effect of Ca-P coating and electrospun fibers in each medium was analyzed.

Effect of Ca-P coating. On day 7, significant upregulation of BMP-2 expression was observed in both coated scaffolds in basic medium. A trend showing upregulation of OP in presence of Ca-P coating was observed in both media, and this upregulation was significant in the 3DF+ESP scaffold group in basic medium. In mineralization medium, the Ca-P coating significantly downregulated the expression of ALP, BSP and OC in 3DF coated scaffolds, while 3DF+ESP coated scaffolds in basic medium had
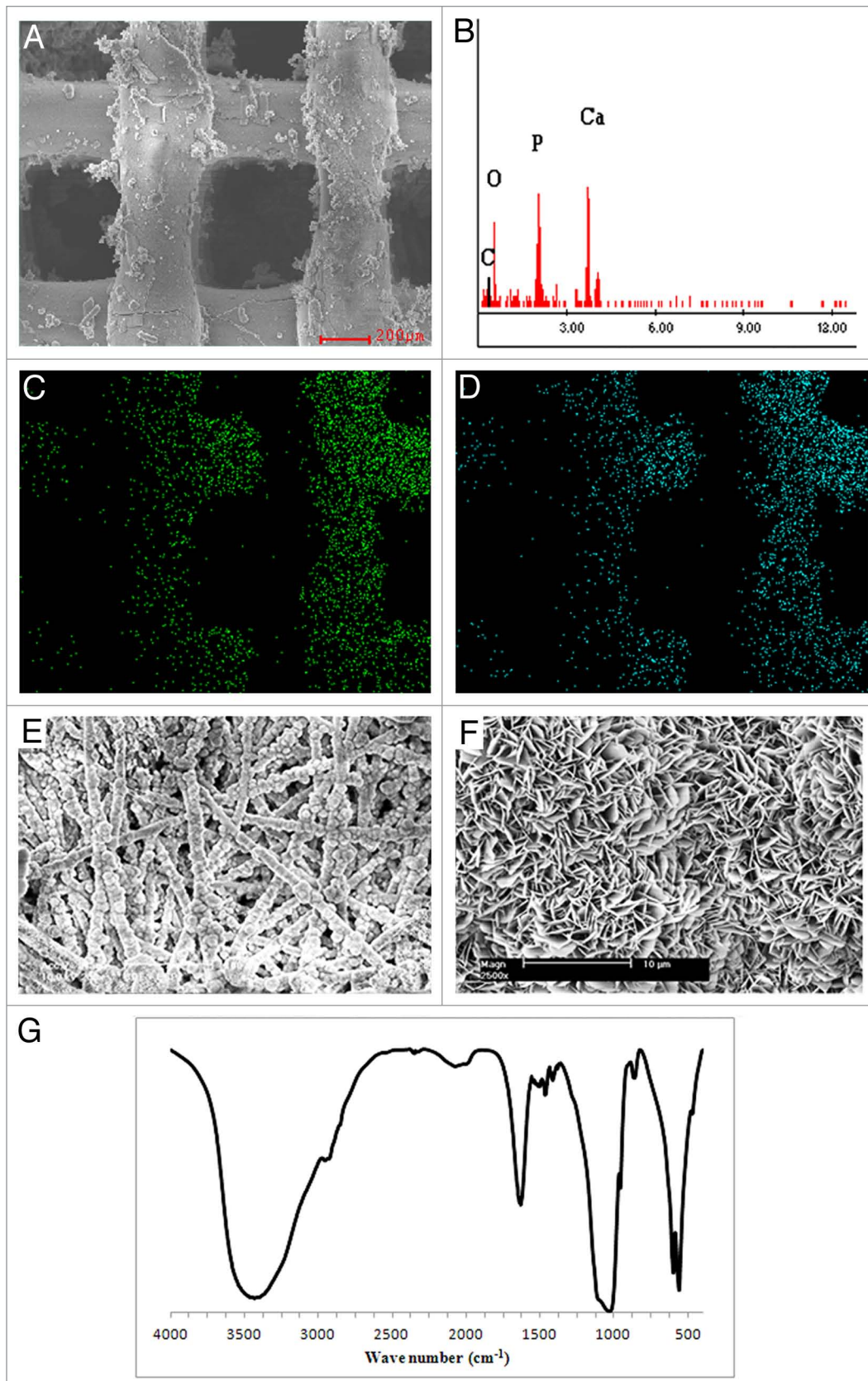
Figure 3. Calcium-phosphate coated rapid prototyped scaffolds. Morphology and characterization. (**A**) SEM image of a 3DF scaffold coated with calcium-phosphate (scale bar = 200 μm). (**B**) EDX spectrum of the scaffold showing Ca and P peaks, (**C and D**) EDX elemental mapping of calcium and phosphorus respectively, (**E**) Electrospun fibers from a 3DF + ESP scaffold that have been coated with calcium-phosphate (scale bar = 100 μm). (**F**) High magnification SEM image showing the morphology of crystals formed during coating (scale bar = 10 μm), (**G**) FT-IR spectrum of calcium-phosphate coating.
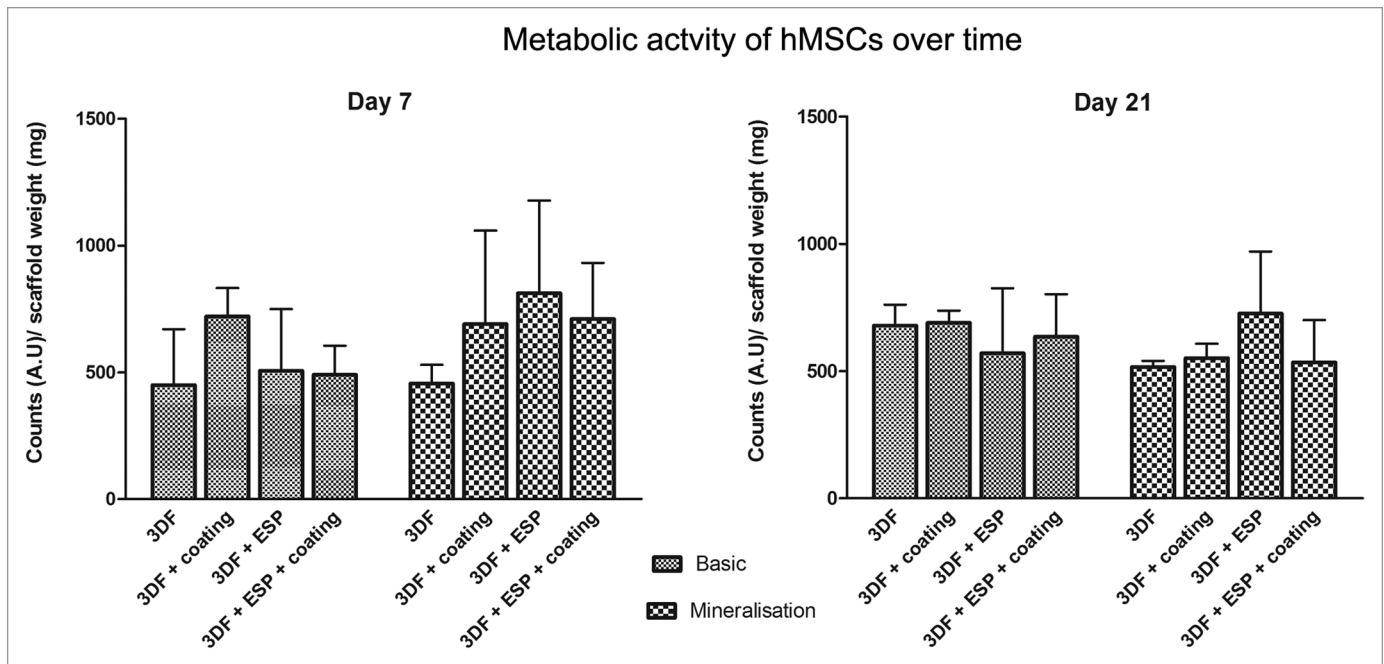
Figure 4. Metabolic activity of cells seeded on different scaffolds in basic and mineralization medium on days 7 and 21 measured using Alamar Blue assay. Data are represented as mean ± standard deviation.

a significantly lower expression of ON compared with 3DF+ESP scaffolds.

On day 21, significant upregulation of BMP-2 and OP was again observed in 3DF coated (basic and mineralization medium) and 3DF + ESP coated (basic medium) scaffolds. OP expression showed nearly 40 and 70 fold induction in coated scaffolds with and without electrospun fibers respectively. Significant downregulation of BSP and ALP expression due to the presence of coating was observed for both sets of coated scaffolds in basic medium.

Effect of electrospun fibers. On day 7, the presence of electrospun fibers led to a significant downregulation in the expression of BSP, ALP and OC in mineralization medium while no significant differences in gene expression of osteogenic markers was observed in the basic medium. On day 21, statistically significant differences in gene expression were observed only for BMP-2 and OP in basic medium. In the presence of Ca-P coating, a positive effect of the electrospun mesh was observed in the case of BMP-2 whereas the addition of an electrospun mesh led to a significantly lower expression of OP. No differences due to the presence of an electrospun mesh were observed in mineralization medium.

Discussion

RP in the form of 3DF deposition was combined with ESP and Ca-P coatings to successfully fabricate hybrid scaffolds for use in bone tissue engineering. Although 3DF and ESP based scaffolds have been separately used for tissue engineering applications, we hypothesized that a combination or merger of these two technologies would lead to improved scaffold properties at different scales. While 3DF scaffolds can provide the necessary mechanical stability[6,37] and support in compression, the ESP scaffolds

serve to mimic the fibrillar nature of ECM and they generally provide a suitable surface for cell attachment. The combination of 3DF and ESP has already shown enhanced cellular response in terms of cell numbers and increased ALP or GAG production when used as a scaffold for bone[19] and cartilage[20] tissue engineering respectively. In an earlier study,[38] we demonstrated the in vivo bone forming ability of Ca-P coated electrospun scaffolds in combination with goat MSCs in a subcutaneous nude mouse model and hence decided to add another layer of functionality to the scaffolds by coating them with Ca-P, thereby providing chemical cues for differentiation. By using biomimetic method based on immersion in an aqueous solution of inorganic salts at near-physiological conditions, we succeeded in homogenously coating both 3DF and 3DF + ESP scaffolds with a layer of Ca-P, that was a mixture of OCP and CA, which are considered precursor and end phase of mineral part of bone[24,39,40] respectively.

All scaffolds allowed the adhesion and proliferation of hMSCs, and at 21 d, ECM production was observed inside the scaffolds. No effect of either ESP mesh or Ca-P coating was found on cell proliferation; however, cell number at 21 d, expressed in terms of total DNA amount, was lower in coated scaffolds containing ESP mesh than in coated 3DF scaffolds. Similarly, in mineralization medium, uncoated 3DF + ESP scaffolds had the highest amount of DNA after 21 d and this amount was significantly higher than that observed in the Ca-P coated 3DF + ESP scaffolds. A possible reason for a significant decrease in DNA amounts in presence of electrospun fibers in the coated scaffolds could be that, after coating, the pore size of the electrospun meshes decreases to a size whereby the cells are trapped in the first electrospun layer at the periphery of the scaffold and therefore do not optimally use the whole scaffold for proliferation. Although in this
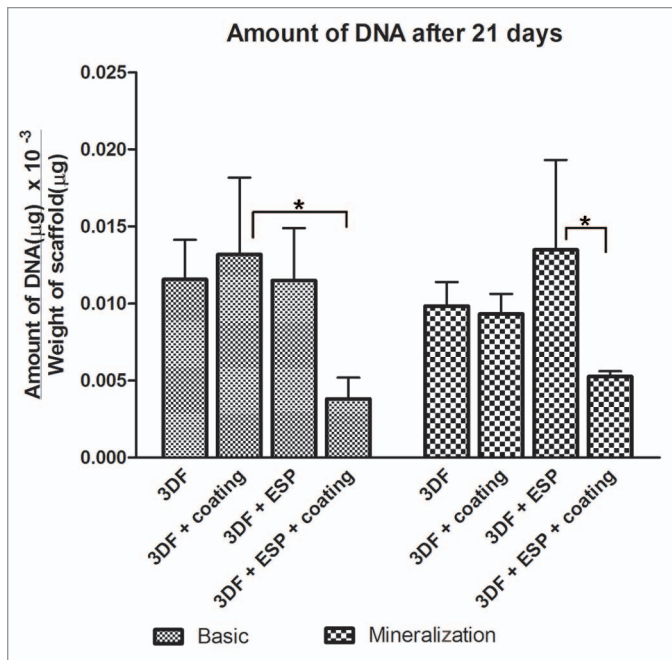
Figure 5. Amount of DNA after 21 d on different scaffolds in basic and mineralization medium as measured using CyQuant assay. Data are represented as mean ± standard deviation. *Statistically significant differences (p < 0.05).

study we did not measure the thickness of the coating, previous studies[41] using electrospun fibers of the same polymer and fiber diameter have shown that this type of coating can reach a thickness of approximately 15 μm. Considering that the pore size between the ESP fibers is about 40 μm, it is indeed possible that the coating has "clogged" the mesh. Decreasing the initial fiber density by reducing the spinning time is a way of obtaining a less dense ESP mesh, which, in this case, would improve interconnectivity of pores throughout the scaffold, thus even through the ESP mesh. Hence, in this study, the hypothesized in vitro benefit of the entrapment of cells inside the ESP mesh was not directly visible, particularly when the scaffolds were coated with Ca-P. In previous studies where RP and ESP technologies were integrated[19,20] to study the behavior of SaOS-2 osteosarcoma cell line and bovine chondrocytes respectively, a higher ratio of electrospun to RP layers (1 ESP layer per 2 RP layers) was used than in the current study (1 ESP layer every 4 RP layers). In these studies, cell proliferation was positively influenced by the presence of ESP fibers at early time points, however, in the study by Moroni et al., a decrease in DNA amounts at later time points was observed, which was explained by the initiation of chondrogenic differentiation of cells. Cell differentiation as a cause of a decrease in cell proliferation was not observed in the present study. Another study that combined RP and ESP showed significant differences in porcine chondrocyte proliferation up to 4 d due to the presence of the electrospun mesh but no difference after 7 d, which was attributed to saturation in cell proliferation within the scaffold.[42] These results suggest that an increase in the number of ESP layers and a decrease of their density as compared with the conditions used in our study should ensure significant

cell retention without closure of pores due to the coating in vitro. It should however be emphasized that in vivo, optimal conditions can be different, given the fact that in vivo, degradation behavior of both polymeric mesh and Ca-P coatings is different too and that additional needs of nutrient supply, blood vessel ingrowth etc. need to be met as well.

The effect of Ca-P coating on cell proliferation depends on many factors like Ca-P phase, crystallinity and therewith related degradation behavior of the coating.[43-46] We previously reported a decrease in DNA amounts in hMSCs on electrospun fibers coated with a Ca-P layer similar to the one used in the present study as compared with the uncoated fibers,[41] which is in accordance with the results obtained here with hybrid 3DF+ESP scaffolds. Different apatite structures[47] seeded with MC3T3-E1 cells showed lower cell number compared with tissue culture plastic after different time points (4 and 14 d) and Anselme and coworkers[43] showed that proliferation of human bone derived cells on plasma sprayed hydroxyapatite (HA) coatings was only possible after prolonged soaking of the coated scaffolds in culture medium. In contrast, PLLA films coated with apatite or collagen/apatite blend showed a significantly higher proliferation of Saos-2 cells compared with bare PLLA films.[48] It is therefore difficult to draw general conclusions on the effect of Ca-P on proliferation of MSCs. In the present study, however, the effect of Ca-P coating on cell number was only visible for hybrid scaffolds, and not for 3DF ones, which indeed suggests that the "clogging" effect caused by physical presence of the Ca-P layer may be of bigger importance that the chemical effect of presence of Ca-P or release of calcium and phosphate ions.

While in vitro studies on combination of ESP and 3D RP scaffolds have been performed,[19,20,42] they have mainly assessed cell proliferation, morphology and biochemical expression of typical markers like ALP and GAG on cell lines or animal derived cells. In order to assess applicability of these technologies in tissue repair and regeneration, experiments with human cells are of importance prior to in vivo testing. Therefore, we seeded our scaffolds with bone marrow derived hMSCs and analyzed the gene expression of various osteogenic markers at two different time points —day 7 and day 21.

The applied Ca-P coating comprises a mixture of OCP and CA, biologically relevant phases of Ca-P. The bioactivity of Ca-P coatings in a bony environment that is believed to originate in degradation of Ca-P is the main reasons for their use in orthopedic and maxillo-facial implants. This degradation leads to an increase in local ion concentration in the vicinity of the implant, resulting in subsequent precipitation of a bone like carbonated apatite on the substrate.[49] Previous studies performed on similar coatings have shown the formation of a carbonated apatitic phase two weeks after an OCP coated Ti plate was placed in α-MEM[49] suggesting that the degradation process starts earlier. In the current experimental set up, the released calcium and/or phosphate ions plausibly affected differentiation of hMSCs. Tada and coworkers observed increased BMP-2 expression[50] in dental pulp cells due to elevated levels of calcium, which is in accordance with our results using hMSCs. Another study[51] showed that at calcium concentrations greater than 6 mM, MC3T3E1
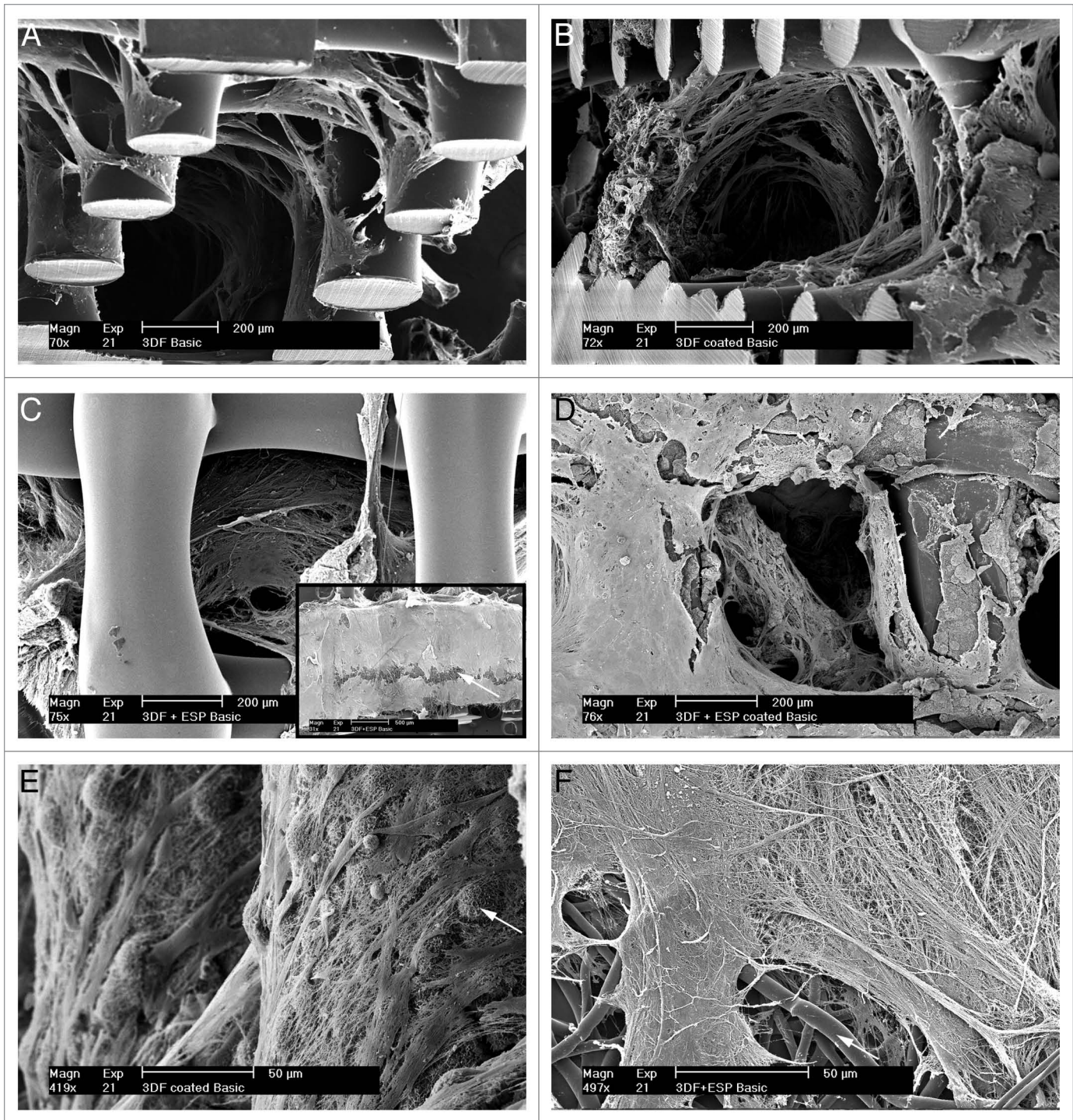
Figure 6. Cell morphology on scaffolds after 21 d. (**A–D**) represent 3DF (uncoated and coated) and 3DF + ESP (uncoated and coated scaffolds) in basic medium. Inset in C shows hMSCs on the electrospun layer (indicated by white arrow). (**E**) Higher magnification image of hMSCs attaching calcium-phosphate coatings. White arrow indicates coating. (**F**) Higher magnification image of hMSCs on electrospun fibers (white arrow). Scale bars **A-D** = 200 μm. Inset in **C** = 500 μm, **E and F** = 50 μm.

osteoblasts showed enhanced mineralization and expression of angiopoietin-1 (Ang-1) that promotes the structural integrity of blood vessels and variation in expression of angiopoietin-2 (Ang-2), a naturally occurring antagonist for promoting blood vessel growth. Besides angiogenic activity, Ang-1 is also involved in osteogenesis and overexpression of Ang-1 led to enhanced ALP activity, OC production and mineralization.[52] Calcium concentration could play a role in osteogenic differentiation and reproducing hematopoetic stem cell niche or bone marrow by controlling the expression of angiopoietin related genes. Our recent results
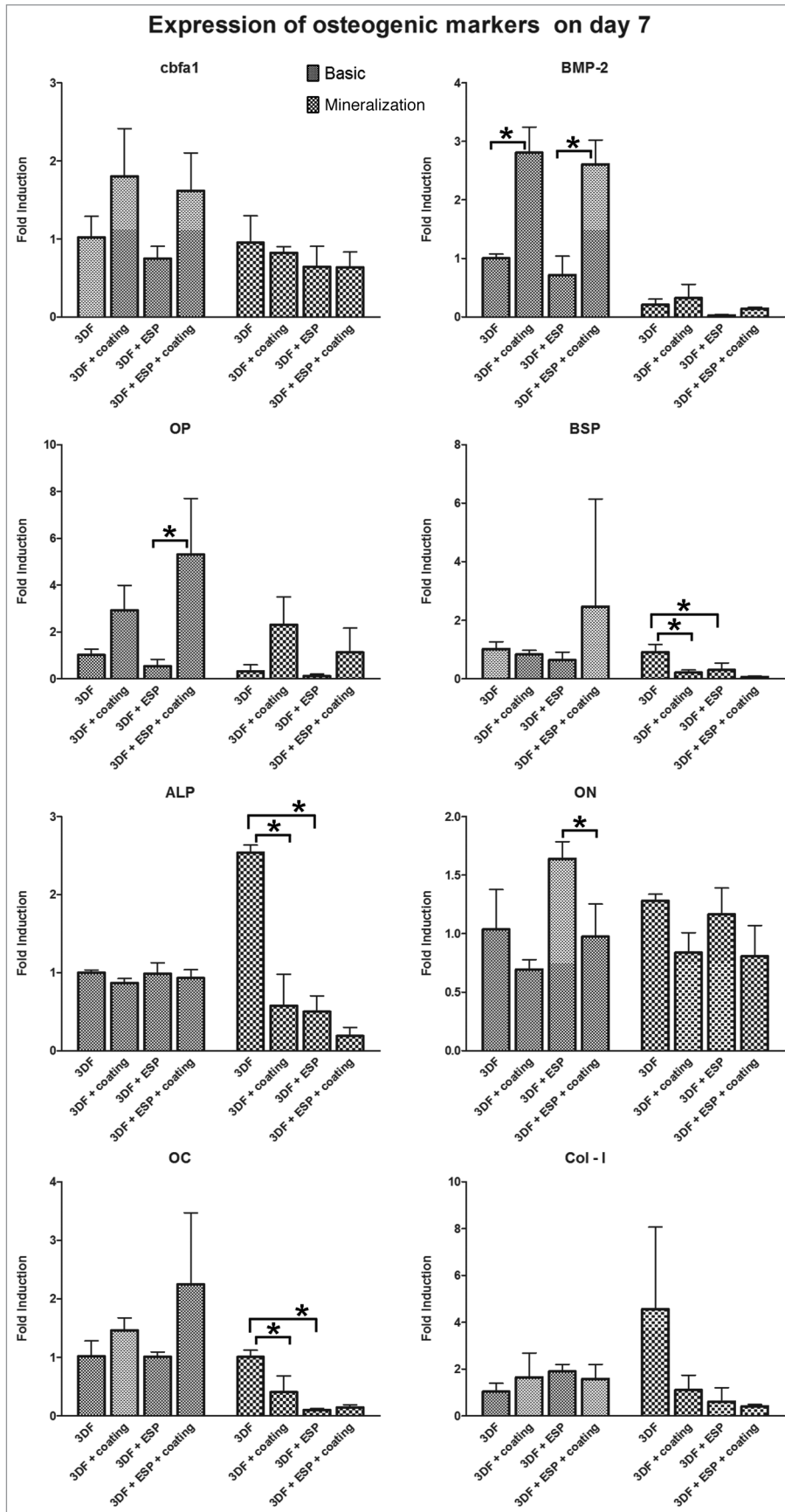
Figure 7. qPCR analysis for osteogenic panel of genes after 7 d in culture. * represents p < 0.05. Data are represented as mean ± standard deviation.
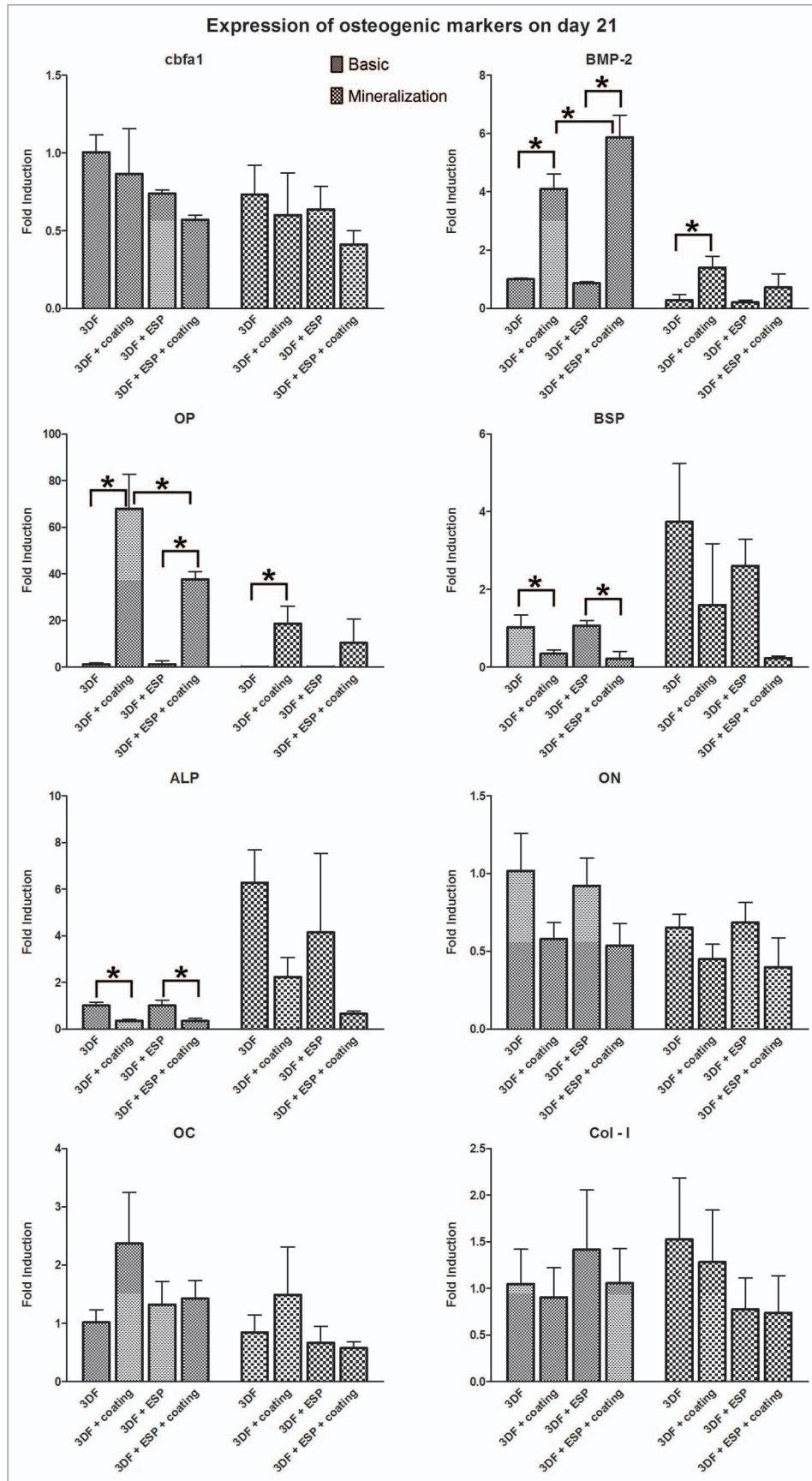
Figure 8. qPCR analysis for osteogenic panel of genes after 21 d in culture. * represents p < 0.05. Data are represented as mean ± standard deviation.

also showed a 3-fold increase in BMP-2 levels in hMSCs after 6 h of culture with 7.8 mM calcium.[53] Besides BMP-2, the gene the expression of which was consistently upregulated in coated scaffolds was OP. The high levels of expression (~40 and 70 fold) are comparable to earlier studies performed on ceramics[54] where OP expression showed a 200,000 fold increase in tricalcium phosphate ceramics compared with cultures on tissue culture plastic. Beck et al.[55] showed that phosphate is a specific signal for inducing OP expression and further elucidated possible signaling pathways for the regulation of OP.[56] Other osteogenic markers like cbfa1, a transcription factor linked to osteoblast proliferation and differentiation and a master switch in the osteogenic differentiation of mesenchymal stromal cells[57] was also upregulated on day 7 in coated scaffolds. Arafat et al.[32] also observed the same trend in cbfa1 expression in porcine MSCs on rapid prototyped PCL-TCP scaffolds coated with carbonated HA on days 17 and 24.

It is interesting to note that most of the observed upregulation of genes due to scaffold modifications (predominantly presence of Ca-P) occurred in basic medium as opposed to the mineralization medium. While this facet needs further investigation, it suggests that standard culturing protocols for 2D cell cultures may not yield the same results when other cues like Ca-P coatings are incorporated into scaffolds.

Materials and Methods

Materials. PolyActive™ (PA) was provided by PolyVation BV, The Netherlands. Following an aPEOTbPBTc nomenclature, the composition used in this study was 300PEOT55PBT45 where, (1) is the molecular weight in g/mol of the starting poly(ethylene glycol) (PEG) blocks used in the copolymerisation, while (2) and (3) are the weight ratios of the PEOT and PBT blocks, respectively. All the salts and reagents used for the preparation of the coating were purchased at either Merck or Sigma-Aldrich.

Fabrication of 3DF scaffolds. 3D scaffolds were fabricated by 3DF using a Bioplotter. The Bioplotter (Envisiontec GmbH, Germany) is an XYZ plotter device as previously described.[58] Briefly, polymer granules were loaded onto a stainless steel syringe and heated at 195°C using a thermostat controlled cartridge unit, fixed on the "X"-mobile arm of the apparatus. A pressure of 4 bars (nitrogen) was applied to the syringe through a pressurised cap once the polymer had melted. Rectangular block models were loaded on the Bioplotter CAM (PrimCAM) software and deposited layer by layer as the polymer was extruded through a nozzle (0.7mm OD) on a stage. The deposition speed was varied between 200–300 mm/min. The spacing between fibers in the same layer was set at 0.8 mm and the layer thickness was 0.225 mm. A 0–90° configuration was used for scaffold architecture where fibers were deposited with 90° orientation steps between successive layers.

Deposition of electrospun fibers onto 3DF scaffolds. PA was dissolved in a mixture of chloroform- hexafluoroisopropanol (HFIP) (78–22%v/v) respectively. A 28% (w/v) PEOT/PBT solution in chloroform- HFIP were prepared and stirred overnight at room temperature. The solution was loaded into a syringe and the flow rate was controlled using a syringe pump (KDS 100,

KD Scientific). The other end of the syringe was connected to a needle, on which a positive high voltage was applied using a high voltage generator (Gamma High Voltage Research Inc.). A metallic sheet of stainless steel was the collector (ground). An electrostatic field was formed between the needle and the collector when the generator was turned on. The polymer solution was pushed through the syringe to the tip of the needle. When the electrostatic field strength overcame the surface tension of the liquid drop at the tip of the needle, the drop was stretched into fibers and deposited onto the 3DF scaffold placed on the collector. A flow rate of 15 mL/h, distance of 15 cm and voltage of 12 kV were used for the spinning and fibers were deposited for 30 sec on the collector. This process was repeated at 0.9 mm, 2.025 mm and 2.925mm of 3DF scaffold height to create 3DF-ESP scaffolds. For the in vitro experiments, configuration 1 ESP layer per 4 3DF layers was selected. Temperature and humidity were monitored during the process and ranged between 19.6–20.4°C and 33–42% respectively.

Preparation of biomimetic Ca-P coatings on scaffolds. 3DF and 3DF-ESP scaffolds were punched to cylinders (5 mm diameter, 4 mm height) and coated with Ca-P using a two-step coating process. In the first step, a five times concentrated simulated body fluid solution (SBF × 5) was prepared by dissolving reagent grade NaCl (40 g), $CaCl_2.2H_2O$ (1.84 g), $MgCl_2.6H_2O$ (1.52 g), $NaHCO_3$ (1.76 g) and $Na_2HPO_4.2H_2O$ (0.89 g) salts in 1l of demineralised water at 37°C under CO_2 gas bubbling. The CO_2 source was then removed from the solution and the 3DF and 3DF-ESP scaffolds were immersed in the solution in a partly open vial and left to coat for 24 h under continuous gentle stirring at 37°C. This process was previously shown to result in a formation of thin, amorphous Ca-P layer.

In the second step, scaffolds pre-coated in step 1 were immersed in a calcium phosphate solution (CPS) at physiological pH of 7.4 and temperature of 37°C for 24 h to deposit a crystalline layer onto previously formed amorphous Ca-P layer. CPS was prepared by dissolving NaCl (8 g), $CaCl_2.2H_2O$ (0.59 g), $Na_2HPO_4.H_2O$ (0.36 g) and Tris (6.05 g) in MilliQ water and the pH of the solution was adjusted to 7.4 with 1M HCl. The coated scaffolds were thoroughly washed in MilliQ water and dried overnight at 50°C.

Characterization of scaffolds. The architecture and composition of the different types of scaffolds were characterized using Environmental SEM in secondary electron mode coupled to EDX analyzer (XL 30 ESEM-FEG, Philips). FTIR spectroscopy (Perkin Elmer Spectrum 1000) was performed on the coatings which were obtained by scratching the coated scaffolds. Fiber diameters were calculated from SEM micrographs using Image J (National Institutes of Health).

HMSC isolation and cell seeding. Bone marrow aspirates were obtained after written informed consent, and hMSCs were isolated and proliferated as described previously.[59] Briefly, aspirates were resuspended by using 20-gauge needles, plated at a density of 5×10^5 cells/cm² and cultured in hMSC proliferation medium containing α-minimal essential medium (Life Technologies), 10% fetal bovine serum (Cambrex), 0.2 mM ascorbic acid (Asap; Life Technologies), 2 mM L-glutamine (Life Technologies), 100

units/ml penicillin (Life Technologies), 10 μg/ml streptomycin (Life Technologies), and 1 ng/ml basic fibroblast growth factor (FGF) (Instruchemie). Cells were grown at 37°C in a humid atmosphere with 5% CO_2. Medium was refreshed twice a week, and cells were used for further sub-culturing or cryopreservation. The hMSC basic medium was composed of hMSC proliferation medium without basic FGF. Mineralization medium was composed of hMSC basic medium with supplemented with 10^{-8} M dexamethasone (Sigma) and 0.01 M β-glycerophosphate (BGP; Sigma). Cells were trypsinised prior to seeding on scaffolds.

The in vitro experiments were performed with cells from one donor at passage 3. Cylinders (5mm diameter, 4mm height) of the four types of scaffolds (3DF, 3DF + coating, 3DF + ESP and 3DF + ESP + coating) were soaked in 70% ethanol for 30 min and dried overnight in a laminar flow cabinet. The scaffolds were washed twice with sterile PBS, transferred to a 25 well non-treated polystyrene plate (Greiner Bio One) and incubated at 37°C in a humid atmosphere with 5% CO_2 for four hours in basic cell culture medium. After removing the medium, each scaffold was seeded with 700,000 cells approximately for PCR analysis and 500,000 cells for Alamar blue and DNA assay in 80 μl basic medium. The cell-scaffold constructs were incubated for three hours to allow cell attachment and topped up to 2 ml with appropriate media. Scaffolds were cultured either in basic media or mineralization media and medium was refreshed twice a week. As a control, T- 25 flasks were seeded at 5,000 cells/cm² in basic and mineralization medium.

Alamar blue assay for cell metabolism. Metabolism was assessed using Alamar blue assay according to the manufacturer's protocol. Briefly, culture medium was replaced with medium containing 10% (v/v) Alamar blue solution (Biosource) and the cells were incubated at 37°C for 4 h. Fluorescence was measured at 590 nm on a Perkin Elmer Victor3 1420 Multilabel plate reader. Proliferation was analyzed on day 7 and 21 and the readout from the scaffolds was corrected with the blank from each group and normalized to scaffold weight.

DNA assay. Scaffolds were washed with PBS and frozen at -80°C overnight. The constructs were then digested at 56°C in a Tris-EDTA buffered solution containing 1 mg/ml proteinase K, 18.5 μg/ml pepstatin A and 1 μg/ml iodoacetamide (Sigma-Aldrich) for 18 h. Cell numbers were determined using the CyQUANT® DNA quantification kit (Invitrogen) with 50 μl of cell lysate according to the manufacturer's protocol. Fluorescence at an excitation wavelength of 480 nm and an emission wavelength of 520 nm was measured using a Perkin Elmer Victor³ 1420 Multilabel plate reader and total amount of DNA was normalized to scaffold weight.

Cell morphology using SEM. On day 21, one sample from each group was used for SEM analysis. The medium was removed and the scaffolds were washed twice with PBS and fixed in 10% formalin for one hour. After rinsing with PBS, the scaffolds were dehydrated in a series of increasing ethanol concentrations (70%, 80%, 90%, 96%, 100% × 2), 15 min in each concentration, before being dried in a critical point dryer (Balzers CPD-030). The samples were then sputter coated with gold (Cressington) for observation on the SEM.

RNA Isolation and gene expression analysis using Quantitative PCR. To analyze the expression of osteogenic markers by hMSCs, total RNA was isolated using a combination of the TRIzol® method with the NucleoSpin®RNA II isolation kit (Macherey-Nagel). Briefly, scaffolds were washed with PBS once and 1ml of TRIzol reagent (Invitrogen) was added to the samples. After one freeze/thaw cylcle, chloroform was added, followed by phase separation by centrifugation, the aqueous phase containing the RNA was collected, mixed with equal volume of 75% ethanol and loaded onto the RNA binding column of the kit. Subsequent steps were in accordance with the manufacturer's protocol. RNA was collected in RNase-free water. The quality and quantity of RNA was analyzed by gel electrophoresis and spectrophotometry. Three hundred ng of RNA were used for first strand cDNA synthesis using iScript (Bio-Rad) according to the manufacturer's protocol. One microliter of undiluted cDNA was used for subsequent analysis. PCR was performed on a Light Cycler real time PCR machine (Roche) using SYBR green I master mix (Invitrogen). Data was analyzed using Light Cycler software version 3.5.3, using the fit point method by setting the noise band to the exponential phase of the reaction to exclude background fluorescence. Expression of osteogenic marker genes was normalized to GAPDH (5'-CGC TCT CTG CTC CTC CTG TT- 3' and 5'-CCA TGG TGT CTG AGC GAT GT-3') levels and fold inductions were calculated using the comparative ΔCT method.[27] The following primer sequences were used for the osteogenic marker genes: Osteocalcin (OC) (5'-GGC AGC GAG GTA GTG AAG AG-3' and 5'-GAT GTG GTC AGC CAA CTC GT-3'), Bone Sialoprotein (BSP) (5'-TGC CTT GAG CCT GCT TCC-3' and 5'-CAA AAT TAA AGC AGT CTT CAT TTT G-3'), Runt-related Transcription Factor-2 (RUNX2/cbfa-1) (5'-GGA GTG GAC GAG GCA AGA GTT T-3' and 5'-AGC TTC TGT CTG TGC CTT CTG G-3'), Collagen type 1 (5'-AGG GCC AAG ACG AAG ACA TC-3' and 5'- AGA TCA CGT CAT CGC ACA ACA-3'), Osteopontin (OP) (5'-CCA AGT AAG TCC AAC GAA AG-3' and 5'-GGT GAT GTC CTC GTC TGT A-3'), Osteonectin (ON) (5'-ACT GGC TCA AGA ACG TCC TG-3' and 5'-GAG AGA ATC CGG TAC TGT GG-3'), and Alkaline Phosphatase (ALP) (5'-GAC CCT TGA CCC CCA CAA T-3' and 5'-GCT CGT ACT GCA TGT CCC CT-3'). For amplification of Bone Morphogenetic Protein-2 (BMP-2), a gene-specific primer mix was used (SA Biosciences), according to the manufacturer's protocol.

Statistical analysis. One way ANOVA with Tukey's multiple comparison post-hoc test was performed. The level of significance was set at 0.05. All data presented are expressed as mean ± standard deviation. Only significant differences due to the effect of coating and presence of electrospun fibers have been shown.

References

1. Hutmacher DW, Schantz T, Zein I, Ng KW, Teoh SH, Tan KC. Mechanical properties and cell cultural response of polycaprolactone scaffolds designed and fabricated via fused deposition modeling. J Biomed Mater Res 2001; 55:203-16; PMID:11255172; http://dx.doi.org/10.1002/1097-4636(200105)55:2<203::AID-JBM1007>3.0.CO;2-7.

2. Williams JM, Adewunmi A, Schek RM, Flanagan CL, Krebsbach PH, Feinberg SE, et al. Bone tissue engineering using polycaprolactone scaffolds fabricated via selective laser sintering. Biomaterials 2005; 26:4817-27; PMID:15763261; http://dx.doi.org/10.1016/j.biomaterials.2004.11.057.

3. Melchels FP, Feijen J, Grijpma DW. A poly(D,L-lactide) resin for the preparation of tissue engineering scaffolds by stereolithography. Biomaterials 2009; 30:3801-9; PMID:19406467; http://dx.doi.org/10.1016/j.biomaterials.2009.03.055.

4. Lopez-Heredia MA, Sohier J, Gaillard C, Quillard S, Dorget M, Layrolle P. Rapid prototyped porous titanium coated with calcium phosphate as a scaffold for bone tissue engineering. Biomaterials 2008; 29:2608-15; PMID:18358527; http://dx.doi.org/10.1016/j.biomaterials.2008.02.021.

5. Sherwood JK, Riley SL, Palazzolo R, Brown SC, Monkhouse DC, Coates M, et al. A three-dimensional osteochondral composite scaffold for articular cartilage repair. Biomaterials 2002; 23:4739-51; PMID:12361612; http://dx.doi.org/10.1016/S0142-9612(02)00223-5.

6. Moroni L, de Wijn JR, van Blitterswijk CA. Three-dimensional fiber-deposited PEOT/PBT copolymer scaffolds for tissue engineering: influence of porosity, molecular network mesh size, and swelling in aqueous media on dynamic mechanical properties. J Biomed Mater Res A 2005; 75:957-65; PMID:16118789; http://dx.doi.org/10.1002/jbm.a.30499.

7. Woodfield TB, Van Blitterswijk CA, De Wijn J, Sims TJ, Hollander AP, Riesle J. Polymer scaffolds fabricated with pore-size gradients as a model for studying the zonal organization within tissue-engineered cartilage constructs. Tissue Eng 2005; 11:1297-311; PMID:16259586; http://dx.doi.org/10.1089/ten.2005.11.1297.

8. Moroni L, Curti M, Welti M, Korom S, Weder W, de Wijn JR, et al. Anatomical 3D fiber-deposited scaffolds for tissue engineering: designing a neotrachea. Tissue Eng 2007; 13:2483-93; PMID:17655485; http://dx.doi.org/10.1089/ten.2006.0385.

9. Dalton PD, Grafahrend D, Klinkhammer K, Klee D, Moller M. Electrospinning of polymer melts: Phenomenological observations. Polymer (Guildf) 2007; 48:6823-33; http://dx.doi.org/10.1016/j.polymer.2007.09.037.

10. Doshi J, Reneker DH. Electrospinning Process and Applications of Electrospun Fibers. J Electrost 1995; 35:151-60; http://dx.doi.org/10.1016/0304-3886(95)00041-8.

11. Li CM, Vepari C, Jin HJ, Kim HJ, Kaplan DL. Electrospun silk-BMP-2 scaffolds for bone tissue engineering. Biomaterials 2006; 27:3115-24; PMID:16458961; http://dx.doi.org/10.1016/j.biomaterials.2006.01.022.

12. Neal RA, McClugage SG, Link MC, Sefcik LS, Ogle RC, Botchwey EA. Laminin nanofiber meshes that mimic morphological properties and bioactivity of basement membranes. Tissue Eng Part C Methods 2009; 15:11-21; PMID:18844601; http://dx.doi.org/10.1089/ten.tec.2007.0366.

13. Ranganath SH, Wang CH. Biodegradable microfiber implants delivering paclitaxel for post-surgical chemotherapy against malignant glioma. Biomaterials 2008; 29:2996-3003; PMID:18423584; http://dx.doi.org/10.1016/j.biomaterials.2008.04.002.

14. Yang F, Murugan R, Wang S, Ramakrishna S. Electrospinning of nano/micro scale poly(L-lactic acid) aligned fibers and their potential in neural tissue engineering. Biomaterials 2005; 26:2603-10; PMID:15585263; http://dx.doi.org/10.1016/j.biomaterials.2004.06.051.

15. Casper CL, Stephens JS, Tassi NG, Chase DB, Rabolt JF. Controlling surface morphology of electrospun polystyrene fibers: Effect of humidity and molecular weight in the electrospinning process. Macromolecules 2004; 37:573-8; http://dx.doi.org/10.1021/ma0351975.

16. De Vrieze S, Van Camp T, Nelvig A, Hagstrom B, Westbroek P, De Clerck K. The effect of temperature and humidity on electrospinning. J Mater Sci 2009; 44:1357-62; http://dx.doi.org/10.1007/s10853-008-3010-6.

17. Deitzel JM, Kleinmeyer J, Harris D, Tan NCB. The effect of processing variables on the morphology of electrospun nanofibers and textiles. Polymer (Guildf) 2001; 42:261-72; http://dx.doi.org/10.1016/S0032-3861(00)00250-0.

18. Moroni L, Licht R, de Boer J, de Wijn JR, van Blitterswijk CA. Fiber diameter and texture of electrospun PEOT/PBT scaffolds influence human mesenchymal stem cell proliferation and morphology, and the release of incorporated compounds. Biomaterials 2006; 27:4911-22; PMID:16762409; http://dx.doi.org/10.1016/j.biomaterials.2006.05.027.

19. Martins A, Chung S, Pedro AJ, Sousa RA, Marques AP, Reis RL, et al. Hierarchical starch-based fibrous scaffold for bone tissue engineering applications. J Tissue Eng Regen Med 2009; 3:37-42; PMID:19021239; http://dx.doi.org/10.1002/term.132.

20. Moroni L, Schotel R, Hamann D, de Wijn JR, van Blitterswijk CA. 3D fiber-deposited electrospun integrated scaffolds enhance cartilage tissue formation. Adv Funct Mater 2008; 18:53-60; http://dx.doi.org/10.1002/adfm.200601158.

21. He DY, Sun XF, Zhao LD. Hydroxylapatite coatings by microplasma spraying. Journal of Inorganic Materials 2007; 22:754-8.

22. Havelin LI, Engesaeter LB, Espehaug B, Furnes O, Lie SA, Vollset SE. The Norwegian Arthroplasty Register: 11 years and 73,000 arthroplasties. Acta Orthop Scand 2000; 71:337-53; PMID:11028881; http://dx.doi.org/10.1080/000164700317393321.

23. Leeuwenburgh S, Layrolle P, Barrère F, de Bruijn J, Schoonman J, van Blitterswijk CA, et al. Osteoclastic resorption of biomimetic calcium phosphate coatings in vitro. J Biomed Mater Res 2001; 56:208-15; PMID:11340590; http://dx.doi.org/10.1002/1097-4636(200108)56:2<208::AID-JBM1085>3.0.CO;2-R.

24. Brown WE. Octacalcium Phosphate and Hydroxyapatite. Nature 1962; 196:1048; http://dx.doi.org/10.1038/1961048b0.

25. Rey C. Calcium phosphate biomaterials and bone mineral. Differences in composition, structures and properties. Biomaterials 1990; 11:13-5; PMID:2397252.

26. Oliveira AL, Mano JF, Reis RL. Nature-inspired calcium phosphate coatings: present status and novel advances in the science of mimicry. Curr Opin Solid St M. 2003; 7:309-18; http://dx.doi.org/10.1016/j.cossms.2003.10.009.

27. Liu YL, Hunziker EB, Layrolle P, De Bruijn JD, De Groot K. Bone morphogenetic protein 2 incorporated into biomimetic coatings retains its biological activity. Tissue Eng 2004; 10:101-8; PMID:15009935; http://dx.doi.org/10.1089/107632704322791745.

28. Liu YL, Layrolle P, van Blitterswijk C, de Groot K. Incorporation of proteins into biomimetic hydroxyapatite coatings. Key Eng Mat 2000; 192:71-4; http://dx.doi.org/10.4028/www.scientific.net/KEM.192-195.71.

29. Kokubo T, Ito S, Huang ZT, Hayashi T, Sakka S, Kitsugi T, et al. Ca,P-rich layer formed on high-strength bioactive glass-ceramic A-W. J Biomed Mater Res 1990; 24:331-43; PMID:2156869; http://dx.doi.org/10.1002/jbm.820240306.

30. Barrere F, van Blitterswijk CA, de Groot K, Layrolle P. Influence of ionic strength and carbonate on the Ca-P coating formation from SBFx5 solution. Biomaterials 2002; 23:1921-30; PMID:11996032; http://dx.doi.org/10.1016/S0142-9612(01)00318-0.

31. Oliveira AL, Costa SA, Sousa RA, Reis RL. Nucleation and growth of biomimetic apatite layers on 3D plotted biodegradable polymeric scaffolds: effect of static and dynamic coating conditions. Acta Biomater 2009; 5:1626-38; PMID:19188103; http://dx.doi.org/10.1016/j.actbio.2008.12.009.

32. Arafat MT, Lam CX, Ekaputra AK, Wong SY, Li X, Gibson I. Biomimetic composite coating on rapid prototyped scaffolds for bone tissue engineering. Acta Biomater 2010; 7:809-20; PMID:20849985.

33. Du C, Meijer GJ, van de Valk C, Haan RE, Bezemer JM, Hesseling SC, et al. Bone growth in biomimetic apatite coated porous Polyactive 1000PEGT70PBT30 implants. Biomaterials 2002; 23:4649-56; PMID:12322986; http://dx.doi.org/10.1016/S0142-9612(02)00214-4.

34. Woodfield TBF, Malda J, de Wijn J, Péters F, Riesle J, van Blitterswijk CA. Design of porous scaffolds for cartilage tissue engineering using a three-dimensional fiber-deposition technique. Biomaterials 2004; 25:4149-61; PMID:15046905; http://dx.doi.org/10.1016/j.biomaterials.2003.10.056.

35. Moroni L, Hamann D, Paoluzzi L, Pieper J, de Wijn JR, van Blitterswijk CA. Regenerating articular tissue by converging technologies. PLoS One 2008; 3:e3032; PMID:18716660; http://dx.doi.org/10.1371/journal.pone.0003032.

36. Du C, Klasens P, Haan RE, Bezemer J, Cui FZ, de Groot K, et al. Biomimetic calcium phosphate coatings on Polyactive 1000/70/30. J Biomed Mater Res 2002; 59:535-46; PMID:11774312; http://dx.doi.org/10.1002/jbm.1267.

37. Moroni L, Poort G, Van Keulen F, de Wijn JR, van Blitterswijk CA. Dynamic mechanical properties of 3D fiber-deposited PEOT/PBT scaffolds: an experimental and numerical analysis. J Biomed Mater Res A 2006; 78:605-14; PMID:16758454; http://dx.doi.org/10.1002/jbm.a.30716.

38. Nandakumar A, Yang L, Habibovic P, van Blitterswijk C. Calcium Phosphate Coated Electrospun Fiber Matrices as Scaffolds for Bone Tissue Engineering. Langmuir 2009; 26:7380-7; PMID:20039599.

39. Brown WE, Eidelman N, Tomazic B. Octacalcium phosphate as a precursor in biomineral formation. Adv Dent Res 1987; 1:306-13; PMID:3504181.

40. Weiner S. Transient precursor strategy in mineral formation of bone. Bone 2006; 39:431-3; PMID:16581322; http://dx.doi.org/10.1016/j.bone.2006.02.058.

41. Nandakumar A, Yang L, Habibovic P, van Blitterswijk C. Calcium phosphate coated electrospun fiber matrices as scaffolds for bone tissue engineering. Langmuir 2010; 26:7380-7; PMID:20039599; http://dx.doi.org/10.1021/la904406b.

42. Kim G, Son J, Park S, Kim W. Hybrid Process for Fabricating 3D Hierarchical Scaffolds Combining Rapid Prototyping and Electrospinning. Macromol Rapid Commun 2008; 29:1577-81; http://dx.doi.org/10.1002/marc.200800277.

43. Anselme K, Sharrock P, Hardouin P, Dard M. In vitro growth of human adult bone-derived cells on hydroxyapatite plasma-sprayed coatings. J Biomed Mater Res 1997; 34:247-59; PMID:9029305; http://dx.doi.org/10.1002/(SICI)1097-4636(199702)34:2<247::AID-JBM14>3.0.CO;2-F.

44. Arinzeh TL, Tran T, Mcalary J, Daculsi G. A comparative study of biphasic calcium phosphate ceramics for human mesenchymal stem-cell-induced bone formation. Biomaterials 2005; 26:3631-8; PMID:15621253; http://dx.doi.org/10.1016/j.biomaterials.2004.09.035.

45. Knabe C, Berger G, Gildenhaar R, Meyer J, Howlett CR, Markovic B, et al. Effect of rapidly resorbable calcium phosphates and a calcium phosphate bone cement on the expression of bone-related genes and proteins in vitro. J Biomed Mater Res A 2004; 69:145-54; PMID:14999762; http://dx.doi.org/10.1002/jbm.a.20131.

46. Midy V, Dard M, Hollande E. Evaluation of the effect of three calcium phosphate powders on osteoblast cells. J Mater Sci Mater Med 2001; 12:259-65; PMID:15348310; http://dx.doi.org/10.1023/A:1008971317544.

47. Chou YF, Huang W, Dunn JC, Miller TA, Wu BM. The effect of biomimetic apatite structure on osteoblast viability, proliferation, and gene expression. Biomaterials 2005; 26:285-95; PMID:15262470; http://dx.doi.org/10.1016/j.biomaterials.2004.02.030.

48. Chen Y, Mak AF, Wang M, Li JS, Wong MS. In vitro behavior of osteoblast-like cells on PLLA films with a biomimetic apatite or apatite/collagen composite coating. J Mater Sci Mater Med 2008; 19:2261-8; PMID:18058196; http://dx.doi.org/10.1007/s10856-007-3335-8.

49. Barrère F, van der Valk CM, Dalmeijer RA, van Blitterswijk CA, de Groot K, Layrolle P. In vitro and in vivo degradation of biomimetic octacalcium phosphate and carbonate apatite coatings on titanium implants. J Biomed Mater Res A 2003; 64:378-87; PMID:12522826; http://dx.doi.org/10.1002/jbm.a.10291.

50. Tada H, Nemoto E, Kanaya S, Hamaji N, Sato H, Shimauchi H. Elevated extracellular calcium increases expression of bone morphogenetic protein-2 gene via a calcium channel and ERK pathway in human dental pulp cells. Biochem Biophys Res Commun 2010; 394:1093-7; PMID:20346918; http://dx.doi.org/10.1016/j.bbrc.2010.03.135.

51. Nakamura S, Matsumoto T, Sasaki J, Egusa H, Lee KY, Nakano T, et al. Effect of calcium ion concentrations on osteogenic differentiation and hematopoietic stem cell niche-related protein expression in osteoblasts. Tissue Eng Part A 2010; 16:2467-73; PMID:20214455; http://dx.doi.org/10.1089/ten.tea.2009.0337.

52. Jeong BC, Kim HJ, Bae IH, Lee KN, Lee KY, Oh WM, et al. COMP-Ang1, a chimeric form of Angiopoietin 1, enhances BMP2-induced osteoblast differentiation and bone formation. Bone 2010; 46:479-86; PMID:19782780; http://dx.doi.org/10.1016/j.bone.2009.09.019.

53. Barradas AM, Fernandes HA, Groen N, Chai YC, Schrooten J, van de Peppel J, et al. A calcium-induced signaling cascade leading to osteogenic differentiation of human bone marrow-derived mesenchymal stromal cells. Biomaterials 2012; 33:3205-15; PMID:22285104; http://dx.doi.org/10.1016/j.biomaterials.2012.01.020.

54. Yuan H, Fernandes H, Habibovic P, de Boer J, Barradas AM, de Ruiter A, et al. Osteoinductive ceramics as a synthetic alternative to autologous bone grafting. Proc Natl Acad Sci U S A 2010; 107:13614-9; PMID:20643969; http://dx.doi.org/10.1073/pnas.1003600107.

55. Beck GR Jr., Zerler B, Moran E. Phosphate is a specific signal for induction of osteopontin gene expression. Proc Natl Acad Sci U S A 2000; 97:8352-7; PMID:10890885; http://dx.doi.org/10.1073/pnas.140021997.

56. Beck GR Jr., Knecht N. Osteopontin regulation by inorganic phosphate is ERK1/2-, protein kinase C-, and proteasome-dependent. J Biol Chem 2003; 278:41921-9; PMID:12920127; http://dx.doi.org/10.1074/jbc.M304470200.

57. Stein GS, Lian JB, van Wijnen AJ, Stein JL, Montecino M, Javed A, et al. Runx2 control of organization, assembly and activity of the regulatory machinery for skeletal gene expression. Oncogene 2004; 23:4315-29; PMID:15156188; http://dx.doi.org/10.1038/sj.onc.1207676.

58. Moroni L, de Wijn JR, van Blitterswijk CA. 3D fiber-deposited scaffolds for tissue engineering: influence of pores geometry and architecture on dynamic mechanical properties. Biomaterials 2006; 27:974-85; PMID:16055183; http://dx.doi.org/10.1016/j.biomaterials.2005.07.023.

59. Both SK, van der Muijsenberg AJC, van Blitterswijk CA, de Boer J, de Bruijn JD. A rapid and efficient method for expansion of human mesenchymal stem cells. Tissue Eng 2007; 13:3-9; PMID:17518576; http://dx.doi.org/10.1089/ten.2005.0513.